

Green Chemistry

Accepted Manuscript



This is an *Accepted Manuscript*, which has been through the Royal Society of Chemistry peer review process and has been accepted for publication.

Accepted Manuscripts are published online shortly after acceptance, before technical editing, formatting and proof reading. Using this free service, authors can make their results available to the community, in citable form, before we publish the edited article. We will replace this *Accepted Manuscript* with the edited and formatted *Advance Article* as soon as it is available.

You can find more information about *Accepted Manuscripts* in the [Information for Authors](#).

Please note that technical editing may introduce minor changes to the text and/or graphics, which may alter content. The journal's standard [Terms & Conditions](#) and the [Ethical guidelines](#) still apply. In no event shall the Royal Society of Chemistry be held responsible for any errors or omissions in this *Accepted Manuscript* or any consequences arising from the use of any information it contains.



www.rsc.org/greenchem

Conversion of cellulose to lactic acid catalyzed by erbium-exchanged montmorillonite K10

Fen-Fen Wang, Jie Liu, Hao Li, Chun-Ling Liu, Rong-Zhen Yang, Wen-Sheng Dong*

Key Laboratory of Applied Surface and Colloid Chemistry (SNNU), MOE, School of Chemistry and Chemical Engineering, Shaanxi Normal University, Xi'an, 710062, China

* To whom correspondence should be addressed.

Phone: +86(0)29-81530806

Fax: +86(0)29-81530806

E-mail: wsdong@snnu.edu.cn

Abstract

Various erbium ion-exchanged montmorillonite K10 materials were prepared by an ion exchange method and were found to act as efficient solid acid catalysts. The catalytic materials synthesized in this work were characterized using a combination of X-ray fluorescence spectroscopy, N₂ adsorption, powder X-ray diffraction, Fourier transform infrared spectroscopy (FT-IR), inductively coupled plasma optical emission spectroscopy, X-ray photoelectron spectroscopy and NH₃ temperature-programmed desorption, as well as by analysis of FT-IR spectra following pyridine adsorption. These catalysts were also evaluated with regard to the hydrothermal conversion of cellulose to lactic acid. Lactic acid yields as high as 67.6% were obtained when reacting 0.3 g cellulose, 0.1 g catalyst and 30 mL water at 240 °C under 2 MPa N₂ for 30 min. Upon recycling of the catalyst, the lactic acid yields decreased from 67.6 to 58.7 to 55.9% during the first, second and third trials. Beginning with the second trial the catalyst behaved as a true heterogeneous catalyst for the conversion of cellulose to lactic acid. The observed decreases in catalytic activity during recycling could be due to a combination of erbium ion leaching, deposition of carbon species in pores and partial structural changes in the catalyst.

Keywords: Cellulose; Lactic acid; Erbium; Montmorillonite K10

1. Introduction

The efficient utilization of renewable resources as liquid fuels and chemicals is becoming a critical issue of global concern in view of the current excessive consumption of fossil resources and the attendant global warming. Renewable resources also represent a means of developing a sustainable development strategy. Cellulose is an abundant, inedible raw material derived from natural biomass; it is renewable and biodegradable and represents a potential resource for the replacement of fossil fuels for the production of bio-based platform chemicals. Hence, there is a significant need for, and significant interest in, devising highly efficient and environment-friendly catalytic routes for converting biomass resources to valuable platform chemicals.¹⁻⁴

Among the various possible biomass derivatives, lactic acid is regarded as a high potential platform chemical for the production of a wide range of useful intermediates such as acrylic acid, propylene glycol, 2,3-pentanedione, acetaldehyde, pyruvic acid and lactides.⁵⁻⁶ It also has extensive applications in pharmaceuticals, the food industry, cosmetics and biodegradable plastics (in the form of polylactic acid) and may also function as an environmentally benign solvent.⁷ The increasing demand for lactic acid will increase the production volumes of this chemical and this represents a significant challenge for both academics and industry. Presently, lactic acid is typically produced *via* biotechnological fermentation of sugars, although this is less than ideal since this process is inefficient, and requires expensive enzymes and a complex purification process.⁵ In view of these drawbacks, it is important to explore alternative chemo-catalytic routes for the production of lactic acid from renewable resources.

Extensive research regarding lactic acid has been conducted in recent years using various materials, such as trioses (dihydroxyacetone, glyceraldehyde),⁸⁻¹¹ glycerol,¹²⁻¹⁵ hexoses,¹⁶⁻²² cellulose and even raw biomass materials as feedstocks.²³⁻³² As an example, Zhang *et al.*²⁷ investigated the hydrothermal conversion of cellulose to lactic acid using Zn, Ni and activated

carbon under alkaline hydrothermal conditions. The highest lactic acid yield of 42% was obtained after 5 min at 300 °C, using 0.02 g Zn, 0.03 g Ni, 0.07 g activated carbon and 2.5 mol/L NaOH. Sanchez *et al.*²⁸ reported the production of lactic acid by hydrothermal treatment of corn cobs in subcritical alkaline water at 300 °C with the addition of 0.7 M Ca(OH)₂, and achieved a maximum yield of 45 mol % of the available (hemi)cellulose in the cobs. Wang *et al.*²⁹ found that PbCl₂ exhibited a remarkable promoting effect on cellulose depolymerization; a lactic acid yield of 68% was achieved by the addition of 0.1 g of ball-milled cellulose (33% crystallinity) to 20 mL water with 0.14 mmol PbCl₂ as the catalyst at 190 °C for 4 h under 3 MPa N₂. More recently, we found that the Lewis acids Er(OTf)₃ and ErCl₃ were able to efficiently catalyze the conversion of micro-crystalline cellulose or raw biomass materials to lactic acid in an aqueous dispersion.^{30,31} Lactic acid yields as high as ~90% were obtained when reacting 0.1 g cellulose, 0.05 g catalyst and 30 mL water at 240 °C under 2 MPa N₂ for 30 min. However, these homogeneous catalysts suffer from difficulty in their separation and recovery from the reaction mixtures. Hence, heterogeneous catalysts are highly desired. Chambon *et al.*³² previously reported cellulose depolymerization using solid Lewis acid catalysts such as tungstated zirconia (ZrW) and alumina (AlW). They generated a lactic acid yield of 27 mol% from 1.6 g cellulose in 65 mL water with 0.68 g AlW as the catalyst at 190 °C for 24 h under 5 MPa He. The yields of lactic acid from the above methods are still far from satisfactory and so the development of an environment-friendly and highly effective heterogeneous catalyst for the conversion of cellulose to lactic acid is still highly desirable.

Montmorillonite is a member of the smectite clay family and has a 2:1 structure, consisting of an octahedral layer of Al sandwiched between two tetrahedral layers of silicon coordinated with oxygen. These crystalline sheets of negatively charged aluminosilicates are balanced by hydrated cations (Na⁺, K⁺ or Ca²⁺) in the interlayer spaces.³³ Montmorillonite K10 clay is a type of acidic stratified silicate mineral with a three-layer structure, and is commercially available at

low cost. It has a large surface area, significant cation-exchange ability, expansible interlayer space, good adsorption capacity, flexible and tunable acidity and is known to be noncorrosive. In addition, it possesses both Lewis and Brønsted acid sites that enable it to function as an alternative catalyst in acid-catalyzed organic transformations with excellent product selectivity.^{34,35} To date, cation-exchanged montmorillonite K10 clays have been used as effective and environmentally benign heterogeneous catalysts or as promising acidic supports for many chemical reactions.³⁶⁻⁴⁰

In the present study, inspired by the excellent catalytic activity of ErCl_3 in the conversion of cellulose to lactic acid and the strong cation exchange ability of montmorillonite K10 clay, we prepared erbium-exchanged montmorillonite K10 clay catalysts and used these materials to catalyze the conversion of cellulose to lactic acid. This novel catalyst shows excellent catalytic performance and great potential for the highly efficient production of lactic acid from cellulose.

2. Experimental

2.1 Chemicals

Microcrystalline cellulose (average particle size of 20 μm) was purchased from Sigma-Aldrich. Formic acid (99%) and acetic acid (99%) were obtained from the Sinopharm Chemical Reagent Co., Ltd. (Shanghai, China). Lactic acid (98%), levulinic acid (98%), erbium chloride (99%) and montmorillonite K10 were purchased from Alfa Aesar. The chemical composition of the montmorillonite K10 was: SiO_2 (79.6%), Al_2O_3 (15.1%), K_2O (1.6%), MgO (1.5%), Fe_2O_3 (1.4%), CaO (0.4%) and TiO_2 (0.3%). All other reagents were analytical grade and were used as-received without further purification.

2.2 Catalyst preparation

The montmorillonite K10 was initially purified by stirring in deionized water at room temperature for 20 h. The resulting slurry was centrifuged, followed by drying at 100 °C for 10

h. The purified montmorillonite K10 (5 g) was then treated with H_2SO_4 (30 wt%, 250 mL) at $100\text{ }^\circ\text{C}$ for 6 h and was subsequently filtered and repeatedly washed with deionized water until the wash water was neutral ($\text{pH} = 7$). Finally, the sample was dried at $110\text{ }^\circ\text{C}$ overnight. The resultant sample was denoted as K10(S).

The erbium ion-exchanged montmorillonite K10 catalysts were prepared by an ion exchange method. In a typical preparation procedure, 1 g of K10(S) was exchanged with 50 mL of ErCl_3 aqueous solution (0.01 mol L^{-1}) at $50\text{ }^\circ\text{C}$ for 24 h with stirring, following which the sample was filtered and washed with deionized water repeatedly, then dried at $110\text{ }^\circ\text{C}$ overnight. The finished product was denoted as Er/K10(S)-1. The other erbium-exchanged montmorillonite catalysts were prepared using the same method described above, but varying the concentration of the aqueous ErCl_3 solution (0.02 , 0.04 and 0.08 mol L^{-1}). These products were denoted as Er/K10(S)-2, Er/K10(S)-3 and Er/K10(S)-4, respectively.

Other metallic ion (Nb^{5+} , Sc^{3+} , In^{3+} , Cr^{3+} , La^{3+} , Nd^{3+} , Sm^{3+} , and Ho^{3+})-exchanged montmorillonite K10 catalysts were prepared using the same method. In each case, 1 g of K10(S) was exchanged with 50 mL of an aqueous MCl_x solution (0.04 mol L^{-1}) at $50\text{ }^\circ\text{C}$ for 24 h with stirring, after which the sample was filtered and washed with deionized water repeatedly and dried at $110\text{ }^\circ\text{C}$ overnight.

2.3 Catalyst characterizations

The relative contents of Er, Si, Al, K, Mg, Ca, Fe, Ti, and Cl in the catalysts were determined using a Shimadzu XRF-1800 X-ray fluorescence spectrometer (40 kV, 95 mA) and more accurate values for Er contents were obtained with a Varian 720-ES inductively coupled plasma optical emission spectrometer (ICP-OES). The crystal structures of the samples were characterized by powder X-ray diffraction using a Rigaku D/MAX-III X-ray diffractometer (35 kV, 40 mA) with a $\text{CuK}\alpha$ source. The diffraction patterns were obtained over the range from 10 to 80° at a scan rate of 8° min^{-1} . The specific surface areas and the pore size distribution of the

samples were obtained by N₂ (−196.2 °C) adsorption measurements using a Micromeritics ASAP 2020M system. Prior to such measurement, the samples were outgassed at 250 °C for 4 h. The surface areas (S_{BET}) of samples were calculated using the BET method and the micropore surface areas (S_{mi}) were obtained using the t -plot method. The mesoporous surface areas (S_{meso}) were determined by subtracting S_{mi} from S_{BET} . Pore size distributions were derived from the desorption branch of the N₂ isotherms using the BJH method, while the total pore volumes (V_{p}) were estimated by considering nitrogen uptake at a relative pressure (P/P_0) of approximately 0.99. The average pore diameter (D_{p}) of each sample was estimated from the surface area and the total pore volume ($D_{\text{p}} = 4V_{\text{p}}/S_{\text{BET}}$). Infrared spectra were recorded on a Thermofisher Nicolet IS10 spectrometer using the KBr disk technique. X-ray photoelectron spectroscopy (XPS) was performed on an Axis Ultra, Kratos (UK) system using an AlK α source (15 kV, 1486.6 eV). The vacuum in the spectrometer was 10^{−9} Torr. The binding energy was calibrated relative to the C1s peak (284.8 eV).

NH₃ temperature-programmed desorption (NH₃-TPD) was performed using a Micromeritics AutoChem II 2920 apparatus equipped with a CirrusTM2 quadrupole mass spectrometry detector. A 100 mg sample was loaded into the sample tube and pretreated in He at 300 °C for 1 h, after which the sample was cooled to 120 °C in a flow of He. Subsequently, a flow of 5% NH₃ in He was introduced and allowed to adsorb at 120 °C for 2 h, following which the sample was purged with dry He at the same temperature to remove the weakly adsorbed NH₃. Finally, the sample was heated at a linear rate of 10 °C min^{−1} under dry He to 800 °C. The desorbed ammonia (m/e=16) was monitored by the quadrupole mass spectrometer.

FT-IR spectra of adsorbed pyridine on the catalyst samples were recorded on a Thermofisher Nicolet IS10 spectrometer, equipped with a deuterium triglycine sulphate detector. Each catalyst sample was compressed into a self-supporting wafer (20 mg, diameter of 13 mm) that was subsequently placed into a quartz IR *in situ* cell equipped with CaF₂ windows. The

wafer was evacuated under vacuum (6×10^{-3} Pa) at 300 °C for 60 min and then cooled to room temperature, followed by exposure to pyridine vapor. The wafer was allowed to adsorb pyridine for 30 min and the IR spectra were recorded at room temperature after subsequent evacuation at 150 °C for 1 h.

2.4 Reaction trials and product analysis

All reactions were performed in a 35 mL stainless steel autoclave equipped with a mechanical stirrer. In a typical experiment, 0.3 g of cellulose, 0.1 g of catalyst and 30 mL water were charged into the reactor, after which the autoclave was purged three times with pure N₂ and then pressurized to 2.0 MPa with N₂ at room temperature. The reaction mixture was heated to 240 °C and held at that temperature for 30 min with stirring at 600 rpm. After each reaction, the reactor was quickly cooled to room temperature using an ice/water mixture and then depressurized, following which the catalyst was separated by centrifugation and filtration. The post-reaction solution was diluted with HPLC mobile phase solution prior to analysis.

Sample analyses were performed on a Shimadzu LC-20AT HPLC system equipped with a RID-10A detector and a Bio-Rad Aminex HPX-87H ion exclusion column (300 × 7.8 mm), using 0.005 M H₂SO₄ as the mobile phase at a flow rate of 0.5 mL min⁻¹. The column temperature was 50 °C and the detector temperature was set to 45 °C. The amount of each product was determined using calibration curves derived from standard solutions.

The cellulose conversion and lactic acid yield were defined as follows.

Cellulose conversion (wt. %):

$$X = \left(1 - \frac{\text{mass of unconverted cellulose}}{\text{mass of initial cellulose}} \right) \times 100\% \quad (1)$$

The yield of product *i* (C %):

$$Y_i = \frac{\text{moles of carbon in product } i}{\text{moles of carbon in initial cellulose}} \times 100\% \quad (2)$$

3. Results and discussions

3.1. Structural characteristics of catalysts

Table 1 shows the relative elemental compositions of the catalysts. The montmorillonite K10 clay contained primarily Al^{3+} with some $\text{Fe}^{2+/3+}$ and Mg^{2+} as octahedral cations and H^+ , Na^+ , K^+ and Ca^{2+} as exchangeable interlayer cations. The treatment of the montmorillonite K10 clay with H_2SO_4 removed mainly octahedral Al cations, together with small amounts of K, Mg, Ca, Fe and Ti. After the exchange with erbium ions, the concentrations of all the other elements are seen to have decreased, although the Si/Al atomic ratio in the catalysts remained almost constant at 10.7 to 12.9, indicating that the erbium ions gradually occupied the interlayer vacancies by replacing H^+ and exchangeable metal ions in the montmorillonite K10 clay interlayers.

The textural properties of the catalysts as determined from nitrogen physisorption are shown in Table 2. The montmorillonite K10 clay had a relatively high specific surface area of $106.2 \text{ m}^2 \text{ g}^{-1}$ and an average pore diameter of 8.4 nm. Following treatment of the clay with H_2SO_4 , the specific surface area decreased to $67.7 \text{ m}^2 \text{ g}^{-1}$ while the average pore diameter increased markedly to 16.4 nm. With increasing erbium ion content in the catalysts, the surface areas evidently decreased significantly, from 61 to $32.7 \text{ m}^2 \text{ g}^{-1}$, whereas the average pore diameter gradually increased to 20.6 nm. The observed reduction in specific surface area may be due to the blockage of pores caused by the introduction of erbium ions.

X-ray diffraction patterns of the samples are shown in Fig. 1, from which it can be seen that the montmorillonite K10 clay exhibits a number of diffraction peaks. The peaks at 19.8° and 34.9° are assigned to the montmorillonite mineral clay, while the peaks at 19.8° , 25.6° , 49.2° and 59.0° are attributed to quartz. The peak at 22.4° is a characteristic diffraction peak of cristobalite and the peaks at 19.8° , 20.8° and 22.4° are ascribed to tridymite-O. These data show

that the montmorillonite K10 was composed of mixed phases, and this result is in good agreement with previously reported data.^{34,36} Treatment of the montmorillonite K10 with H₂SO₄ did not have a marked effect on its phase structure. With increasing erbium ion concentrations in the samples, the intensity of the diffraction peaks at 19.8°, 20.8° and 25.6° decreased, but the typical layered structure of montmorillonite K10 was still observed. The decrease in the intensity of the diffraction peaks at 19.8°, 20.8° and 25.6° could be due to leaching of Al from the octahedral layers of the montmorillonite K10. Fig. 1 also shows that, as the erbium ion content increased, a number of new diffraction peaks appeared at 12.7°, 16.1°, 18.8°, 29.3°, 33.1°, 36.7°, 37.9° and 43.3°, which are a good match for phase-X1, corundum and cronstedtite-1M. This is probably due to that the displacement of small cations such as H⁺, Fe³⁺, Al³⁺ by Er³⁺ and the swelling of montmorillonite layers. However, no diffraction peaks resulting from erbium compounds were observed, indicating that the erbium ions were highly dispersed throughout these catalysts.

The FT-IR spectra of the samples are shown in Fig. 2. The overall spectral features of K10(S) and erbium-exchanged montmorillonite K10 are quite similar to those of pure montmorillonite K10. In the case of pure montmorillonite K10, the most intense band at 1110 cm⁻¹ is attributed to Si–O out-of-plane stretching, while the shoulder at 1035 cm⁻¹ is due to the Si–O in-plane stretching vibration and the weak band at 527 cm⁻¹ is due to the Si–O bending vibration in the tetrahedral sheets.^{40,41} The broad bands at 3623 and 1639 cm⁻¹ correspond to the stretching and bending vibrations of the hydroxyl groups of water molecules present in the clay. The band at 915 cm⁻¹ is due to the AlAlOH bending vibration, while the band at 793 cm⁻¹ is assigned to the platy form of disordered tridymite and the bands at 692 and 469 cm⁻¹ are most likely due to the presence of quartz.^{40,41} After treatment of the montmorillonite K10 with H₂SO₄ and exchange with erbium ions, the adsorption bands at 3623 cm⁻¹, due to hydroxyl groups bonded with Al³⁺ cations, and at 1637 cm⁻¹, due to bending vibrations of the hydroxyl groups,

both show a remarkable decrease with increasing erbium ion content, suggesting that the amount of water molecules coordinated to the octahedral cations in the clay decreased, possibly resulting in a decrease in Brønsted acidity. In addition, the intensities of the Si–O bending vibration at 527 cm^{-1} , the bridging hydroxyl group mode at 915 cm^{-1} and the shoulder of the Si–O band at 1035 cm^{-1} in the tetrahedral sheets all gradually weaken and even disappear, indicating changes in the Si and Al in the surrounding environment. However, the bands at 1110 cm^{-1} assigned to the Si–O stretching vibration and at 793 cm^{-1} assigned to the platy form of disordered tridymite do not obviously change, indicating that the tetrahedral silicon layers are basically stable. The band at 3536 cm^{-1} is attributed to nonacidic hydroxyl groups. In addition to the band at 3536 cm^{-1} , a new band at 625 cm^{-1} , assigned to the Er–Cl bond, is observed in the erbium-exchanged montmorillonite K10 clays. The intensity of this band is seen to increase with increasing erbium content, suggesting that partial deposition of ErCl_3 may have occurred in the clay interlayers and was not removed fully by water washing.

XPS analysis showed that the erbium-exchanged montmorillonite K10 catalysts contained only Er, Al, Si, O and C, no Cl element was detected, further confirming that excess ErCl_3 was deposited in the clay interlayers. $\text{Er}4d_{5/2}$ XPS profiles of the various erbium-exchanged catalysts are shown in Fig. 3. The $\text{Er}4d_{5/2}$ binding energy (BE) for all samples was 168.8 eV, which is equal to the BE value of Er (168.8 eV) in Er_2O_3 and ErCl_3 , indicating that the Er in the erbium-exchanged catalysts was present as Er(III).

3.2. Acidic characteristics of the catalysts

The total acidity of each catalyst was determined by the NH_3 -TPD-MS method, and the results are summarized in Fig. 4. The montmorillonite K10 clay showed a small desorption peak centered at approximately $150\text{ }^\circ\text{C}$, followed by a relatively strong, broad NH_3 desorption peak ranging from 350 to $600\text{ }^\circ\text{C}$, indicating that the surface of this sample featured two different types of acidic sites: weak and strong. In the case of the K10(S), the quantities of both weak and

strong acidic sites were reduced, owing to the removal of Al from the octahedral layer of the montmorillonite K10 and the coordination of water molecules to octahedral cations resulting from the H₂SO₄ treatment. The surface acidity was significantly enhanced as erbium ion were incorporated into the montmorillonite K10 interlayers by ion exchange, although the NH₃ desorption peak shifted towards lower temperatures concurrent with the decrease in strong acid sites, indicating that there were substantial amounts of weak acid sites on the surfaces of the erbium-exchanged catalysts. With increasing Er contents in the samples, the quantity of acid sites gradually increased. The Er/K10(S)-3 had a lower number of weakly acidic sites but more strongly acidic sites compared to the Er/K10(S)-4, as indicated by the larger NH₃ desorption peak exhibited around 620 °C by the Er/K10(S)-3. The reason for this is unclear and requires further investigation.

Fig. 5 presents IR spectra of the various catalysts following pyridine adsorption. In the case of the montmorillonite K10 clay, the peak at 1445 cm⁻¹ arising from the C–C stretching vibration of the coordination-bonded pyridine complex indicates the presence of Lewis acid sites. The small peak at 1540 cm⁻¹, attributed to the C–C stretching vibration of the pyridinium ion (PyH⁺), shows the presence of a lesser amount of Brønsted acid sites, and the peak at approximately 1490 cm⁻¹ was assigned to pyridine adsorbed on both Lewis and Brønsted acid sites.^{33,36} These results suggest that the montmorillonite K10 contained primarily Lewis acid sites together with a lower concentration of Brønsted acid sites. Following treatment of the montmorillonite K10 with H₂SO₄, the peak at 1445 cm⁻¹ decreased in intensity, suggesting that the amount of Lewis acid sites on the K10(S) was lowered. In comparison with K10(S), the intensities of the peaks at 1445 cm⁻¹ and 1540 cm⁻¹ of Er/K10(S)-1, Er/K10(S)-2 and Er/K10(S)-3 did not exhibit marked changes, indicating that these four catalysts had similar amounts of strong acidic sites capable of adsorbing pyridine molecules. With further increases in the concentration of erbium ions, the intensities of the peaks at 1445 and 1540 cm⁻¹ are seen to

decrease, indicating that the Er/K10(S)-4 had the lowest concentration of accessible acidic sites among all the samples owing to its minimal specific surface area.

3.3. Catalytic activity

The hydrothermal conversion of cellulose was assessed using these montmorillonite catalysts, with the results shown in Table 3. In the presence of the montmorillonite K10, the cellulose was fully converted but no lactic acid was detected in the product mixture. The main products were rather 5-hydroxymethylfurfural (HMF), with a yield of 24.2%, and glucose, with a yield of 11.5%, together with lesser amounts of formic acid, levulinic acid, acetic acid, acetol and glyceraldehyde. The catalytic activity of the montmorillonite K10 clay can be explained in terms of its Lewis and Brønsted acid sites. The Brønsted acidity in this material is mainly associated with the hydrated cations in the interlamellar regions, and the Lewis acidity results from cations on the edge sites.⁴² The Brønsted acid sites are able to catalyze the hydrolysis of cellulose to glucose, while the Lewis acid sites catalyze the isomerization of glucose to fructose.⁴³ HMF is formed by the dehydration of fructose, catalyzed by both Brønsted and Lewis acid sites.⁴⁴ The HMF can, in turn, be rehydrated to formic and levulinic acids. The organic acids in the product mixture are generated through degradation of fructose or glucose and also *via* HMF.⁴⁵

The K10(S) had a similar product distribution to that obtained from the montmorillonite K10, although the yields of HMF and glucose were higher, with 26.1 and 17.9% yields, respectively. NH₃-TPD results showed that the montmorillonite K10 had a higher concentration of strong acid sites than the K10(S), while the pyridine adsorption IR spectra indicated that the montmorillonite K10 contained a greater quantity of Lewis acid sites. Therefore, the lower yields of glucose and HMF generated when employing the montmorillonite K10 could be due to promotion of the carbonization of cellulose and intermediates by the strong acid sites on the montmorillonite K10 at higher temperatures (240 °C), thus decreasing the yields of glucose and

HMF.

When using the erbium-exchanged montmorillonite K10 as the catalyst, lactic acid was clearly detected in the product mixture, with yields higher than 40%, suggesting that the erbium ions played a key role in the conversion of cellulose to lactic acid. Our previous results demonstrated that erbium ions can coordinate with the hydroxyl groups on cellulose rings, owing to the higher electron densities at these sites. This results in easier cleavage of the protonated ether bonds between the two glucosyl units in the soluble oligosaccharide intermediates that are formed by the depolymerization of cellulose catalyzed by the hydroxonium ions present in the aqueous medium at 240 °C.^{30,31} As a result, the erbium ions promote the conversion of soluble oligosaccharides to lactic acid.

As the concentration of erbium ions in the catalysts was increased, the yields of lactic acid initially increased and then decreased, indicating that a low concentration of active sites produces a low yield of lactic acid, while overly high active site concentrations lead to further reaction of the lactic acid to undesirable products, thus decreasing the yield. Among these catalysts, the Er/K10(S)-3 generated the highest yield of lactic acid (67.6%). As present, it is not possible to establish a direct correlation between the catalytic performance and the surface acidity as measured by the NH₃-TPD data and pyridine adsorption IR spectra of the erbium-exchanged catalysts. This is because it was determined that some erbium ions were dissolved in the reaction solvents, and these dissolved erbium ions could also have contributed to the conversion of cellulose to lactic acid. In order to identify the role of the montmorillonite, 0.038 g of ErCl₃, containing the same number of moles of Er as 0.1 g of the Er/K10(S)-3, was also employed to catalyze the conversion of cellulose. The results showed that the cellulose was again completely converted under these conditions, with a lactic acid yield of 69.6% (close to the yield obtained with the Er/K10(S)-3 catalyst). A mixture of 0.038 g of ErCl₃ with 0.0767 g of K10(S), containing the same mass of K10(S) as 0.1 g Er/K10(S)-3, was also used as a catalyst,

and the results showed that this catalytic system generated a lactic acid yield and a product distribution similar to those obtained with pure ErCl_3 . These data suggest that the K10(S) clay does not have a marked effect on the conversion of cellulose in the present system, but rather serves primarily as a support to anchor the active erbium ions.

The reusability of the Er/K10(S)-3 in the conversion of cellulose to lactic acid was also investigated. After each reaction, the catalyst was separated from the reaction solution by centrifugation, filtered, washed with deionized water and dried at 100 °C overnight before the next run. The data in Table 4 indicate that the yield of lactic acid obtained from the Er/K10(S)-3 decreased sharply over the course of the initial two recycling trials; the yield dropped from an initial value of 67.6 to 58.7% for the 2nd run, and then decreased slightly to 55.9% for the 3rd run. ICP-OES analysis confirmed that, following the first run, 5.2% of the Er had leached from Er/K10(S)-3 while, during the following recycling trials, only a trace amount of Er was leached from the catalyst. These results suggest that, following the initial trial, the Er/K10(S)-3 behaved as a true heterogeneous catalyst for the conversion of cellulose to lactic acid.

As shown in Table 4, the yield of lactic acid decreased over the course of the recycling trials. The yield of HMF also increased, suggesting that modification of the Er/K10(S)-3 occurred. It is known that the acidity of cation-exchanged montmorillonite is influenced by the quantity of water retained between its clay layers.⁴² Brønsted acidity results from the reaction shown below.³³



Here x is the number of water molecules directly bonded to the metal cation M , and $m+$ is the charge on the cation. In this manner, the hydrated cations in the interlayer space are dissociated, producing protons and thus Brønsted acidity. During recycling it is very likely that

the Brønsted acidity of the Er/K10(S)-3 was increased through the insertion of water molecules between the clay layers, whereas its Lewis acidity was decreased owing to the leaching of erbium ions. The increased Brønsted acidity could promote the hydrolysis of the cellulose to glucose, followed by the isomerization of glucose and the dehydration of fructose to HMF. The reduced Lewis acidity would decrease the direct conversion of the soluble oligosaccharide intermediates to lactic acid without proceeding through glucose intermediates.³¹

To determine the reasons underlying the apparent catalyst deactivation, the used catalyst was characterized by XRD, FT-IR, XPS and ICP and also subjected to BET analysis. The XRD pattern (see Fig. s1) of the used catalyst did not show remarkably change as compared with the fresh Er/K10(S)-3. Both the fresh and used catalysts show similar FT-IR spectra in Fig. 6, but the bands at 793, 625 and 469 cm^{-1} are decreased in intensity following use, indicating that some structural changes occurred in the Er/K10(S)-3 during the reaction. Moreover, XPS analysis (see Fig. s2) showed the oxidation state of Er did not change after reaction, but the intensity of Er 4d peak decreased, indicating the content of Er in the used catalyst decreased. Besides, the carbon content in the used catalyst increased from 20.8 to 43.4%. BET analysis revealed that the specific surface area of the Er/K10(S)-3 fell from 47.6 to 30.5 $\text{m}^2 \text{g}^{-1}$ after three recycling trials. Hence, the observed decrease in catalytic activity during recycling could be due to a combination of the leaching of erbium ions and the deposition of carbon species in the clay pores, together with structural changes in the Er/K10(S)-3.

In addition to the Er/K10(s) catalysts, K10 specimens exchanged with other metal cations, including Nb^{5+} , Sc^{3+} , In^{3+} , Cr^{3+} , La^{3+} , Nd^{3+} , Sm^{3+} , and Ho^{3+} were also prepared. These metal cation exchanged montmorillonite catalysts showed similar XRD patterns with the montmorillonite K10 clay, and no new phase was detected (see Fig. s3). They were also used as catalysts for the conversion of cellulose to lactic acid. The results presented in Table 5 indicate that these Nb^{5+} , Sc^{3+} , In^{3+} , and Cr^{3+} exchanged montmorillonite catalysts exhibited very

different catalytic activities for the conversion of cellulose. The main products were glucose and HMF, together with lesser amounts of formic acid, levulinic acid, lactic acid, acetol, glyceraldehyde and some brown, insoluble polymer. These results indicate that the catalytic activity strongly depends on the interlayer exchanged cations. For the La^{3+} , Nd^{3+} , Sm^{3+} , and Ho^{3+} exchanged montmorillonite catalysts, the yield of lactic acid increased gradually with decreasing metallic cation radius. Previously, we also examined the catalytic activities of homogeneous lanthanide triflates for the hydrothermal conversion of cellulose to lactic acid, and similar trend was also observed.³⁰ However, it was strange that we found ~20% yields of HMF and ~4% yields of glucose were obtained over these La^{3+} , Nd^{3+} , Sm^{3+} , and Ho^{3+} exchanged montmorillonite catalysts. Whereas, in the case of the Er/K10(s)-3, only 3.7% yields of HMF were obtained, and none of glucose was detected. The reason is unclear and needs to be further investigated in detail.

4. Conclusion

We have demonstrated that erbium ion-exchanged montmorillonite K10 can effectively catalyze the conversion of cellulose to lactic acid. The montmorillonite does not have a significant influence on the catalytic activity as such, but rather serves primarily as a support to anchor the active erbium ions. Lactic acid yields as high as 67.6% were obtained when reacting 0.3 g cellulose, 0.1 g Er/K10(S)-3 catalyst and 30 mL water at 240 °C under 2 MPa N_2 for 30 min. During recycling, the yield of lactic acid decreased gradually while the HMF yield increased, suggesting that the surface acidity of the Er/K10(S)-3 was modified. The decreased catalytic activity following recycling could be due to the combined effects of leaching of erbium ions, deposition of carbon species in the clay pores, and structural changes in the catalyst.

Acknowledgments

The authors gratefully acknowledge financial support from the Program for Key Science and Technology Innovation Team of Shaanxi Province (2012KCT-21), the Program for Changjiang Scholars and Innovative Research Team in University of China (IRT_14R33), and the Fundamental Research Funds for the Central Universities (GK201305011).

References

- 1 D.M. Alonso, J.Q. Bond, J.A. Dumesic, *Green Chem.*, 2010, **12**, 1493–1513.
- 2 P. Gallezot, *Chem. Soc. Rev.*, 2012, **41**, 1538–1558.
- 3 A. Wang, T. Zhang, *Acc. Chem. Res.*, 2013, **46**, 1377–1386.
- 4 J. Song, H. Fan, J. Ma, B. Han, *Green Chem.*, 2013, **15**, 2619–2635.
- 5 M. Dusselier, P.V. Wouwe, A. Dewaele, E. Makshina, B.F. Sels, *Energy. Environ. Sci.*, 2013, **6**, 1415–1442.
- 6 F. Jin, H. Enomoto, *Energy. Environ. Sci.*, 2011, **4**, 382–397.
- 7 R. Datta, M. Henry, *J. Chem. Technol. Biotechnol.*, 2006, **81**, 1119–1129.
- 8 Y. Hayashi, Y. Sasaki, *Chem. Commun.*, 2005, 2716–2718.
- 9 J.C. Wang, Y. Masui, M. Onaka, *Appl. Catal. B: Environ.*, 2011, **107**, 135–139.
- 10 C.B. Rasrendra, B.A. Fachri, I.G. Makertihartha, S. Adisasmito, H.J. Heeres, *ChemSusChem*, 2011, **4**, 768–777.
- 11 F. de Clippel, M. Dusselier, R. Van Rompaey, P. Vanelderren, J. Dijkmans, E. Makshina, L. Giebeler, S. Oswald, G.V. Baron, J.F.M. Denayer, P.P. Pescarmona, P.A. Jacobs, B.F. Sels, *J. Am. Chem. Soc.*, 2012, **134**, 10089–10101.
- 12 C.A. Ramírez-López, J.R. Ochoa-Gómez, M. Fernández-Santos, O. Gómez-Jiménez-Aberasturi, *Ind. Eng. Chem. Res.*, 2010, **49**, 6270–6278.

- 13 J. Xu, H. Zhang, Y. Zhao, B. Yu, S. Chen, Y. Li, L. Hao, Z. Liu, *Green Chem.*, 2013, **15**, 1520–1525.
- 14 X. Jin, L. Dang, J. Lohrman, B. Subramaniam, S. Ren, R.V. Chaudhari, *ACS Nano*, 2013, **7**, 1309–1316.
- 15 R.K.P. Purushothaman, J. van Haveren, D.S. van Es, I. Melián-Cabrera, J.D. Meeldijk, H.J. Heeres, *Appl. Catal. B: Environ.*, 2014, **147**, 92–100.
- 16 M.S. Holm, S. Saravanamurugan, E. Taarning, *Science*, 2010, **328**, 602–605.
- 17 G. Epane, J.C. Laguerre, A. Wadouachi, D. Marek, *Green Chem.*, 2010, **12**, 502–506.
- 18 M.S. Holm, Y.J. Pagan-Torres, S. Saravanamurugan, A. Riisager, J.A. Dumesic, E. Taarning, *Green Chem.*, 2012, **14**, 702–706.
- 19 A. Onda, T. Ochi, K. Kajiyoshi, K. Yanagisawa, *Catal. Commun.*, 2008, **9**, 1050–1053.
- 20 Z. Liu, W. Li, C. Pan, P. Chen, H. Lou, X. Zheng, *Catal. Commun.*, 2011, **15**, 82–87.
- 21 C.B. Rasrendra, I.G.B.N. Makertihartha, S. Adisasmito, H.J. Heeres, *Top. Catal.*, 2010, **53**, 1241–1247.
- 22 Q. Guo, F. Fan, E.A. Pidko, W.N. van der Graaff, Z. Feng, C. Li, E.J. Hensen, *ChemSusChem*, 2013, **6**, 1352–1356.
- 23 X.Y. Yan, F.M. Jin, K. Tohji, A. Kishita, H. Enomoto, *AIChE J.*, 2010, **56**, 2727–2733.
- 24 F.W. Wang, Z.B. Huo, Y.Q. Wang, F.M. Jin, *Res. Chem. Intermed.*, 2011, **37**, 487–492.
- 25 L.Z. Kong, G.M. Li, H. Wang, W.Z. He, F. Ling, *J. Chem. Technol. Biotechnol.*, 2008, **83**, 383–388.
- 26 W.P. Deng, Q.H. Zhang, Y. Wang, *Catal. Today*, 2014, **234**, 31–41.
- 27 S. Zhang, F. Jin, J. Hu, Z. Huo, *Bioresour. Technol.*, 2011, **102**, 1998–2003.
- 28 C. Sanchez, I. Eguees, A. Garcia, R. Llano-Ponte, J. Labidi, *Chem. Eng. J.*, 2012, **181**, 655–660.
- 29 Y.L. Wang, W.P. Deng, B.J. Wang, Q.H. Zhang, X.Y. Wan, Z.C. Tang, Y. Wang, C. Zhu, Z.X. Cao, G.C. Wang, H.L. Wan, *Nature Commun.*, 2013, **4**, 2141–2148.
- 30 F.F. Wang, C.L. Liu, W.S. Dong, *Green Chem.*, 2013, **15**, 2091–2195.

- 31 X. Lei, F.F. Wang, C.L. Liu, R.Z. Yang, W.S. Dong, *Appl. Catal. A: Gen.*, 2014, **482**, 78–83.
- 32 F. Chambon, F. Rataboul, C. Pinel, A. Cabiac, E. Guillon, N. Essayem, *Appl. Catal. B: Environ.*, 2011, **105**, 171–181.
- 33 A. Jha, A.C. Garade, M. Shirai, C.V. Rode, *Appl. Clay. Sci.*, 2013, **74**, 141–146.
- 34 G.B.B. Varadwaj, S. Rana, K. Parida, *Chem. Eng. J.*, 2013, **215–216**, 849–858.
- 35 Z.F. Fang, B. Liu, J.J. Luo, Y.S. Ren, Z.H. Zhang, *Biomass. Bioenergy*, 2014, **60**, 171–177.
- 36 K.I. Shimizu, T. Higuchi, E. Takasugi, T. Hatamachi, T. Kodama, A. Satsuma, *J. Mol. Catal. A: Chem.*, 2008, **284**, 89–96.
- 37 V.V. Bokade, G.D. Yadav, *Appl. Clay. Sci.*, 2011, **53**, 263–271.
- 38 J. Wang, J. Ren, X. Liu, J. Xi, Q. Xia, Y. Zu, G. Lu, Y. Wang, *Green Chem.*, 2012, **14**, 2506–2512.
- 39 B.S. Kumar, A. Dhakshinamoorthy, K. Pitchumani, *Catal. Sci. Technol.*, 2014, **4**, 2378–2396.
- 40 B. Tyagi, C.D. Chudasama, R.V. Jasra, *Spectrochi. Acta, Part A*, 2006, **64**, 273–278.
- 41 P. Kumar, R. V. Jasra, T.S.G. Bhat, *Ind. Eng. Chem. Res.*, 1995, **34**, 1440–1448.
- 42 L. Jankovič, P. Komadel, *J. Catal.*, 2003, **218**, 227–233.
- 43 Y. Román-Leshkov, M.E. Davis, *ACS Catal.*, 2011, **1**, 1566–1580.
- 44 S. Dutta, S. De, B. Saha, *Biomass. Bioenergy*, 2013, **55**, 355–369.
- 45 J.B. dos Santos, F.L. da Silva, F.M.R. Sobral Altino, T. da Silva Moreira, M.R. Meneghetti, S.M.P. Meneghetti, *Catal. Sci. Technol.*, 2013, **3**, 673–678.

Table 1. The relative compositions of catalysts as determined by XRF.

Catalyst	Content (wt %)								
	Er ^a	Si	Al	K	Mg	Ca	Fe	Ti	Cl
K10	—	77.2	12.4	4.0	1.2	0.88	3.32	0.68	—
K10(S)	—	76.7	6.2	4.1	0.3	0.33	2.28	0.46	—
Er/K10(S)-1	11.3 (5.6)	75.8	6.1	3.9	—	0.28	0.81	0.44	1.35
Er/K10(S)-2	21.8 (10.3)	68.4	5.1	—	—	0.23	0.47	0.34	3.44
Er/K10(S)-3	34.9 (23.2)	53.2	4.7	—	—	0.19	0.47	0.26	5.99
Er/K10(S)-4	47.9 (29.4)	38.7	3.5	—	—	—	0.38	—	9.12

^aThe values in parentheses represent Er concentrations measured by ICP-OES.

Table 2. The specific surface areas and porous structural parameters of the catalysts.

Catalyst	S_{BET} ($\text{m}^2 \text{g}^{-1}$)	S_{meso} ($\text{m}^2 \text{g}^{-1}$)	V_{p} ($\text{cm}^3 \text{g}^{-1}$)	V_{meso} ($\text{cm}^3 \text{g}^{-1}$)	D_{p} (nm)
K10	106.2	89.9	0.22	0.21	8.4
K10(S)	67.7	47.8	0.28	0.26	16.4
Er/K10(S)-1	61.0	50.4	0.23	0.22	15.4
Er/K10(S)-2	54.7	42.7	0.22	0.21	16.0
Er/K10(S)-3	47.6	38.6	0.20	0.19	17.0
Er/K10(S)-4	32.7	16.4	0.17	0.15	20.6

Table 3. Cellulose conversions obtained with various catalysts.^a

Catalyst	Conversion (%)	Yield (%)							
		Lactic acid	Formic acid	Levulinic acid	Acetic acid	Acetol	HMF	Glyceraldehyde	glucose
ErCl ₃ ^b	100	69.6	3.8	2.5	0.9	5.2	1.6	3.3	0.3
ErCl ₃ + K10(S) ^c	100	69.8	4.0	2.9	1.0	5.1	0.8	4.9	-
K10	100	1.8	1.5	0.9	-	1.4	24.2	0.8	11.5
K10(S)	100	2.2	1.6	1.3	-	1.0	26.1	2.0	17.9
Er/K10(S)-1	100	44.9	2.9	1.3	2.1	4.2	8.8	3.9	-
Er/K10(S)-2	100	63.1	6.1	3.9	2.2	5.6	4.8	5.1	-
Er/K10(S)-3	100	67.6	6.0	3.8	2.3	5.5	3.7	5.4	-
Er/K10(S)-4	100	61.7	2.2	2.0	2.4	4.8	2.2	6.1	-

^aReaction conditions: cellulose 0.3 g, catalyst 0.1 g, H₂O 30 mL, 240 °C, 2 MPa N₂, 30 min.

^bErCl₃ catalyst 0.038 g.

^cErCl₃ catalyst 0.038 g + 0.0767 g K10(S).

Table 4. Cellulose conversions obtained on recycling of the Er/K10(S)-3 catalyst.

Run	Erbium content (wt%)	Conversion (%)	Yield (%)						
			Lactic acid	Formic acid	Levulinic acid	Acetic acid	Acetol	HMF	Glyceraldehyde
1	23.2	100	67.6	6.0	3.8	2.3	5.5	3.7	5.4
2	18.0	100	58.7	3.6	0.8	0.5	3.3	14.1	2.6
3	17.9	100	55.9	3.8	2.1	0.6	2.9	18.9	3.2

Reaction conditions: 0.3 g cellulose, 0.1 g catalyst, 30 mL H₂O, 240 °C, 2 MPa N₂, 30 min.

Table 5. Cellulose conversions obtained with various metal cation-exchanged montmorillonite catalysts.

Catalyst	Conversion (%)	Yield (%)						
		Glucose	HMF	Lactic acid	Levulinic acid	Formic acid	Acetol	Glyceraldehyde
Nb/K10(S)	100	10.9	16.9	7.5	1.2	2.5	2.2	2.4
Sc/K10(S)	100	13.5	23.1	—	2.0	1.4	4.8	1.6
In/K10(S)	100	13.9	22.5	4.2	0.7	1.1	1.6	1.1
Cr/K10(S)	100	16.5	23.8	2.9	0.7	1.2	1.3	2.1
La/K10(S)	100	5.9	23.2	30.9	0.5	1.7	1.7	3.3
Nd/K10(S)	100	4.6	22.1	42.5	0.6	2.0	2.1	2.7
Sm/K10(S)	100	4.1	20.6	48.7	0.5	1.9	2.0	2.3
Ho/K10(S)	100	3.8	22.5	53.6	0.7	2.1	2.1	2.8

Reaction conditions: cellulose 0.3 g, catalyst 0.1 g, H₂O 30 mL, 240 °C, 2 MPa N₂, 30 min.

Figure Captions:

Fig. 1. X-ray diffraction patterns of various catalysts: a) K10, b) K10(S), c) Er/K10(S)-1, d) Er/K10(S)-2, e) Er/K10(S)-3 and f) Er/K10(S)-4.

Fig. 2. FTIR spectra of various catalysts: a) K10, b) K10(S), c) Er/K10(S)-1, d) Er/K10(S)-2, e) Er/K10(S)-3 and f) Er/K10(S)-4.

Fig. 3. Er 4d XPS profiles of various catalysts: a) Er/K10(S)-1, b) Er/K10(S)-2, c) Er/K10(S)-3 and d) Er/K10(S)-4.

Fig. 4. NH₃-TPD-MS curves of various catalysts: a) K10, b) K10(S), c) Er/K10(S)-1, d) Er/K10(S)-2, e) Er/K10(S)-3 and f) Er/K10(S)-4.

Fig. 5. FTIR spectra following the adsorption of pyridine on various catalysts: a) K10, b) K10(S), c) Er/K10(S)-1, d) Er/K10(S)-2, e) Er/K10(S)-3 and f) Er/K10(S)-4.

Fig. 6. FTIR spectra of Er/K10(S)-3 before and after use.

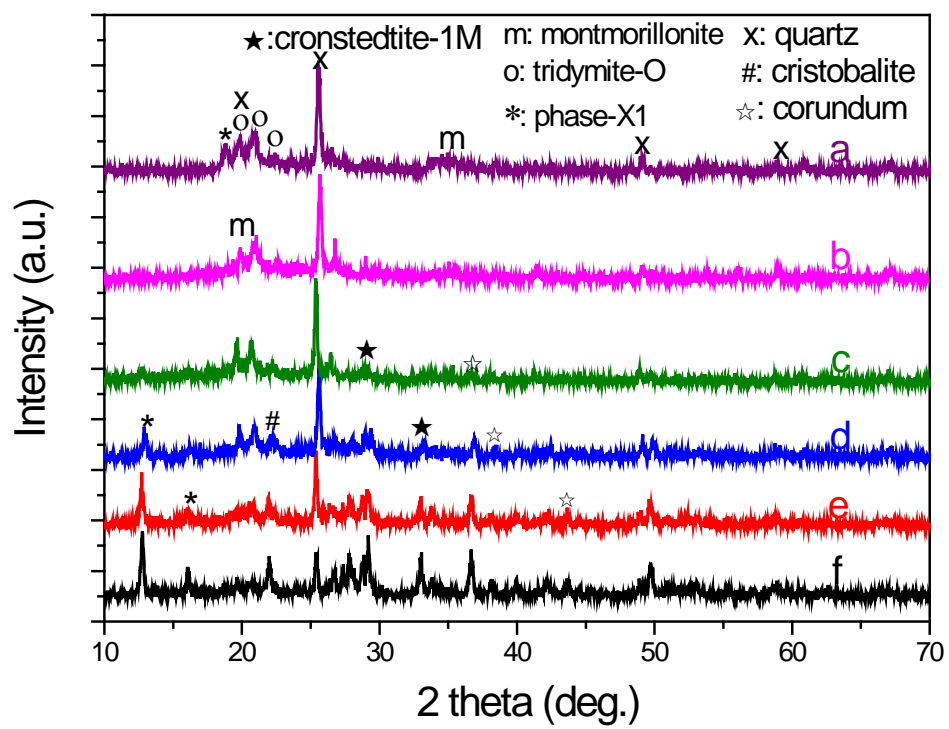
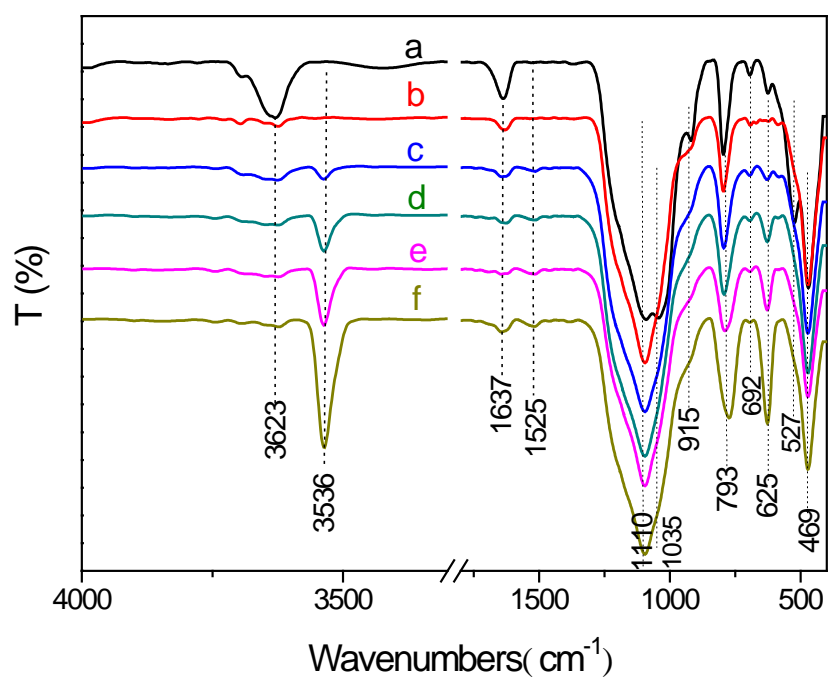


Figure 1

**Figure 2**

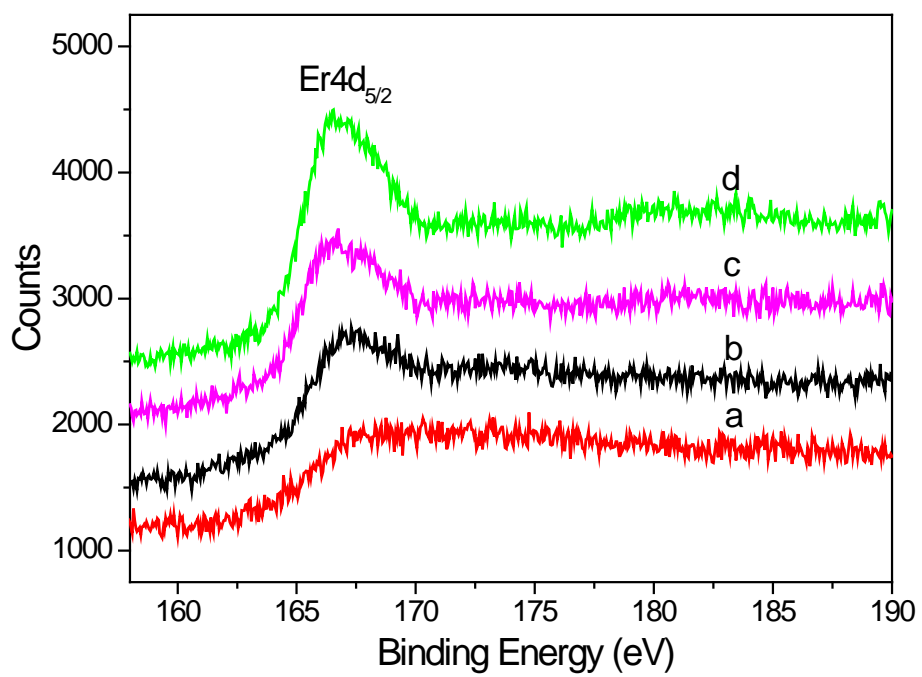
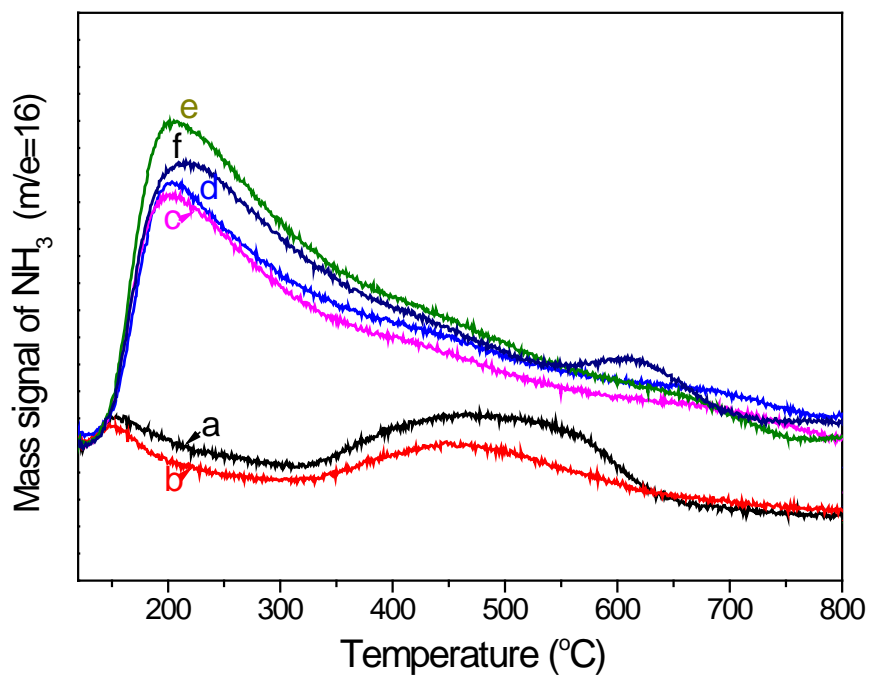
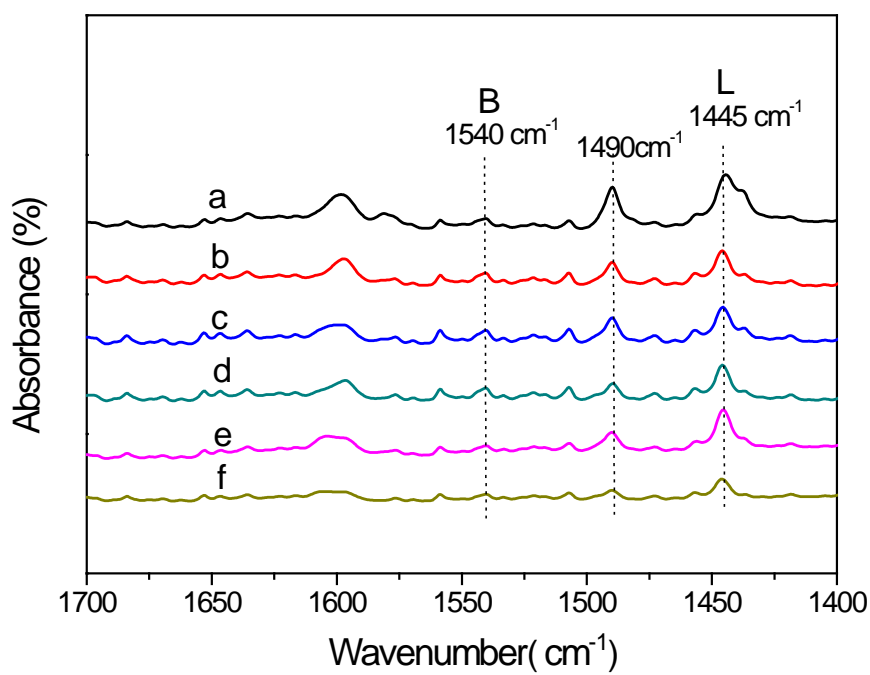
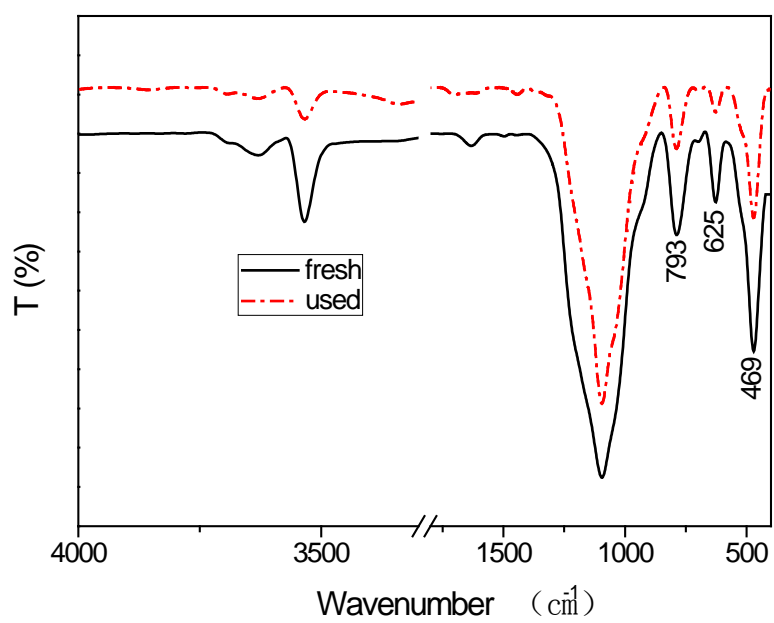


Figure 3

**Figure 4**

**Figure 5**

**Figure 6**

Graphical abstract

Erbium ion-exchanged montmorillonite K10 can catalyze effectively the hydrolysis of cellulose into lactic acid, giving a lactic acid yield as high as 67.6%.

